

available at [www.sciencedirect.com](http://www.sciencedirect.com)journal homepage: [www.elsevier.com/locate/aca](http://www.elsevier.com/locate/aca)

# Understanding the concept of concentration-dependent red-shift in synchronous fluorescence spectra: Prediction of $\lambda_{\text{SFS}}^{\text{max}}$ and optimization of $\Delta\lambda$ for synchronous fluorescence scan

O. Divya, Ashok. K. Mishra\*

Department of Chemistry, Indian Institute of Technology Madras, Chennai-600036, India

## ARTICLE INFO

### Article history:

Received 1 August 2008

Received in revised form

18 September 2008

Accepted 24 September 2008

Published on line 7 October 2008

### Keywords:

Concentration-dependent red-shift

Inner-filter effect

Multifluorophoric systems

Synchronous fluorescence

## ABSTRACT

The phenomenon of concentration-dependent red-shift of fluorescence, observed in multifluorophoric systems at high concentrations, has been successfully used in the analytical fluorimetry of systems like petroleum derivatives, humic substances, biological fluids, etc. From a detailed investigation of the phenomenon, it is inferred that the primary cause contributing to this phenomenon is the inner-filter effect especially under right angle sample geometry condition. In this work, a method based on inner-filter effect has been proposed to obtain an optimal  $\Delta\lambda$  which give the most intense synchronous fluorescence spectral maximum for solutions containing fluorophores at higher concentrations. The applicability of the method has been evaluated for some single fluorophoric samples (coumarin-152, quinine sulphate, rhodamine-6G and fluorescein) at high concentrations. The proposed formula and methodology were applied to certain multifluorophoric systems like diesel, transformer oil and humic acid.

© 2008 Elsevier B.V. All rights reserved.

## 1. Introduction

Analytical fluorimetry with right angle sample geometry works well when the sample absorbance at the excitation wavelength is low (e.g. at low concentrations of the analyte) because of the linear dependence of fluorescence intensity with concentration. But when the absorbance is high (as for samples at high concentrations), the regular variation of intensity with concentration is lost mainly due to inner-filter effects [1,2] and right angle geometry becomes unusable for analytical applications. Thus, there have been many attempts at correcting inner-filter effects [3,4]. For highly concentrated samples, synchronous fluorescence spectroscopy (SFS) with right angle geometry was found to be highly advanta-

geous and has been used successfully for many analytical applications [5–8].

The phenomenon of concentration-dependent shift of synchronous fluorescence spectra has been profitably used to advantage the analysis of certain multifluorophoric systems. Analytical techniques have been developed using this context for the concentrated multifluorophoric samples. Petroleum products, one of the common multifluorophoric systems, have been widely investigated. John and Soutar used synchronous excitation spectrofluorimetry for the identification of crude oils and they observed that, the  $\lambda_{\text{max}}$  of the normal and synchronous excitation spectra showed a marked shift to longer wavelengths as the concentration of the solutions increased [5]. At high concentrations, the excitation energy continue to

\* Corresponding author. Tel.: +91 44 22574207; fax: +91 44-22574202.

E-mail address: [mishra@iitm.ac.in](mailto:mishra@iitm.ac.in) (Ashok.K. Mishra).

0003-2670/\$ – see front matter © 2008 Elsevier B.V. All rights reserved.

doi:10.1016/j.aca.2008.09.056

cascade to larger fluorophores, producing greater red-shifts in the emission spectra due to extensive energy transfer [9,10]. Ralston et al. studied the quantum yields of crude oils, where they have found that dilute solutions of light crude oils exhibit higher quantum yields than those of heavy crude oils [11]. Although they did not carry out any detailed investigation in to the cause of the phenomenon, they postulated that energy transfer processes becomes more probable at higher concentrations and emissions occurs predominantly from highly conjugated molecules.

The first report on red-shift cascade effect in three-dimensional fluorescence spectra was by Smith and Sinski when they investigated the concentration-dependent wavelength shifts in three-dimensional fluorescence spectra of petroleum samples [12]. As the solution strength is decreased, three-dimensional fluorescence maxima systematically shifted to shorter wavelengths. They describe the effect as 'cascade' effect, thereby implying excited state energy transfer to be the primary cause of the red-shift. Sinski et al. utilized the three-dimensional fluorescence red-shift cascade effect to monitor mycobacterium PRY-1 degradation of aged petroleum [13].

Patra and Mishra independently observed a similar behavior when they studied the synchronous fluorescence scan parameters of certain petroleum products [7,8]. They documented that the excitation energy transfer results in shifting of synchronous fluorescence maxima with increasing concentration of the petroleum product. The correlation of this shift with concentration showed the possibility of using it as an analytical method to quantify the petroleum products in the environment. Kao et al. reported a comparison of fluorescence inner-filter effects for different cell configurations for anthracene solutions [14]. They observed that the right angle geometry exhibited the widest linear dynamic range and lowest detectable anthracene concentrations. The effect of sample geometry (front surface illumination, 45° and 90°) on synchronous fluorimetric analysis of petroleum products at a higher concentration was studied [7]. The 90°-angle sample geometry was found to give better analytical utility because it provided certain distinct characteristics to SFS spectra due to extensive inner-filter effect and resonance energy transfer. The observed higher sensitivity with right angle geometry immediately suggests that inner-filter effects play a significant role in the phenomenon of concentration-dependent red-shifts. Other energy degrading interactions like excited state energy transfer and quenching may also be contributing factors.

The concentration-dependent investigation of motor oils like diesel, petrol, kerosene, 2T oil and mobil showed a red-shift in  $\lambda_{\text{SFS}}^{\text{max}}$  [8,15]. With dilution, the total synchronous fluorescence spectral (TSFS) contour maps measured at right-angle geometry of neat diesel samples shifted towards blue (shorter wavelengths) [16]. The total fluorescence spectra (TFS) of certain petroleum products like petrol and diesel produced a blue shift in the excitation and/or emission maximum on dilution with cyclohexane or kerosene [15,17–19]. It has been concluded that the shift is a combined effect of various photo-physical processes such as resonance energy transfer, inner-filter effects, collisional fluorescence quenching, excimer or exciplex formation, etc.

The relative importance of inner-filter effect vis-à-vis other energy degrading mechanisms in causing concentration-dependent red-shift of concentrated multifluorophoric solutions have not been investigated in detail so far. An attempt to investigate this would necessarily involve understanding the inner-filter effects of selected single fluorophores at high concentrations where the effects of other energy degrading processes are negligible. In the first part of the work, fluorescence of single molecules (fluorophores) at high concentration has been studied. Subsequently, the developed method has been applied to certain multifluorophoric systems like diesel, transformer oil and humic acid.

## 2. Materials and methods

### 2.1. Selection of fluorophores

For the initial studies, four fluorophores (quinine sulphate, rhodamine 6G, coumarin 152 and fluorescein) were selected which have different absorption and emission profiles. It is known that these molecules do not form excimers at high concentrations. Characteristics of the fluorescent molecules selected for the study are the following:

- Molecules showing a narrow absorption spectrum (e.g. rhodamine 6G) and a broad absorption spectrum (e.g. quinine sulphate and coumarin 152).
- Molecules with large Stokes' shift (e.g. quinine sulphate and coumarin 152) and small Stokes' shift (e.g. rhodamine 6G and fluorescein).
- Absorption spectrum showing a slow rise (e.g. quinine sulphate and coumarin 152) and a steep rise (e.g. rhodamine 6G and fluorescein).

The absorption, excitation and emission spectra of the above mentioned fluorophores are given in Fig. S1 (Supporting Information).

### 2.2. Sample preparation

Coumarin 152 and humic acid (Cat: H16752) were purchased from Aldrich Chemical Company, USA. Rhodamine 6G, fluorescein and quinine sulphate were purchased from SD fine chemicals. Diesel was collected from the authorized local vendors in Chennai. Transformer oil sample was supplied by Raj Lubricants, Chennai under the trade name of electrol. All the solvents used were of spectroscopic grade.

The stock solutions (0.05 M) of coumarin 152, rhodamine 6G and fluorescein were prepared in ethanol and serial dilutions were done for the preparation of desired concentrations. The stock solution of quinine sulphate (0.05 M) was prepared in 0.1N sulphuric acid. The highest concentration to be used for the study was fixed from the solubility of the compound in the respective solvent and the nature of absorption spectra. A series of concentration ranging from  $5 \times 10^{-2}$  M to  $1 \times 10^{-4}$  M of coumarin 152 and quinine sulphate,  $1 \times 10^{-2}$  M to  $1 \times 10^{-4}$  M of fluorescein and rhodamine, were prepared.

Samples with different relative fractions of diesel (in %, v/v) ranging from 5% to 100% were prepared in hexane by

adding appropriate volumes of diesel to hexane. Transformer oil samples were prepared in the concentration range of 5–100%. Humic acid stock solution ( $1000 \text{ mg L}^{-1}$ ) was prepared in triply distilled water and further dilutions were done ( $50\text{--}1000 \text{ mg L}^{-1}$ ).

### 2.3. Experimental

A PerkinElmer lambda 25 UV–vis spectrophotometer was used for the absorbance measurements. Fluorescence spectra were obtained on a Hitachi F-4500 spectrofluorimeter with a 100 W xenon lamp as excitation source and Jobin-Yvon-Spex Fluorolog II spectrofluorimeter, with a 450 W xenon lamp as light source. For SFS measurement, the scan speed was  $240 \text{ nm s}^{-1}$  and PMT voltage was fixed at 700 V. Band pass for both excitation and emission monochromators were kept at 5 nm. SFS was measured in the excitation wavelength range of 250–650 nm. The derived absorbance data were generated and plotted using Origin 6.0 software.

## 3. Results and discussion

### 3.1. An expression for fluorescence intensity at the centre of the cuvette

In conventional right angle geometry, the fluorescence is usually observed from a volume at the centre of the cuvette. Although the fluorescence intensity is expected to vary along the light path in this observation volume, it can be assumed that for a cuvette of pathlength  $\ell$ , the intensity of incident light at a pathlength of  $\ell/2$  (at the centre of the cuvette) will determine the fluorescence intensity. For a highly concentrated single fluorophoric sample, the longest wavelength edge of the absorbance spectrum is expected to look like Fig. 1.

At longer wavelengths where the absorbance is low, practically no fluorescence is observed. Excitation at shorter wavelengths with absorbance values more than 2 results in front-face fluorescence and low-fluorescence intensity

observed at right angle geometry. Hence, the fluorescence intensity is expected to be maximum at some wavelength at which absorbance is optimal at the centre of the cuvette.

In conventional fluorescence measurement with right angle geometry, an expression explaining the fluorescence intensity at the centre of the cuvette can be derived as follows.

Along the path of a monochromatic incident light, the fluorescence intensity ( $F_\ell$ ) at a pathlength ' $\ell$ ' from the front surface is proportional to (a) the intensity of incident light ' $I_\ell$ ' at that pathlength, (b) the molar extinction coefficient ' $\epsilon$ ' and (c) the fluorescence quantum yield ( $\phi_f$ ).

$$F_\ell = I_\ell \cdot \epsilon \cdot \phi_f \quad (1)$$

The variation of incident light intensity along the light path is given by the Beer-Lambert law:

$$I_\ell = I_0 10^{-\epsilon c \ell} \quad (2)$$

Substituting,

$$F_\ell = I_0 \cdot \epsilon \cdot \phi_f \cdot 10^{-\epsilon c \ell} \quad (3)$$

At fluorophore concentration ' $c$ ' and for a cuvette of unit pathlength, ' $\epsilon$ ' can be substituted by  $(A/c)$ , where ' $A$ ' denotes the absorbance. Thus,

$$F_\ell = I_0 \cdot \frac{A}{c} \cdot \phi_f \cdot 10^{-\epsilon c \ell} \quad (4)$$

A schematic depiction of this expression is given in Fig. 2.

For a particular single fluorophoric system, in the absence of energy degrading effects,  $\phi_f$  is constant. Although fluorescence lifetime measurements have not been carried out in this work, such measurements would be of great help in testing for the constancy of  $\phi_f$ . The above expression can be rewritten to include the variation of fluorescence intensity with wave-

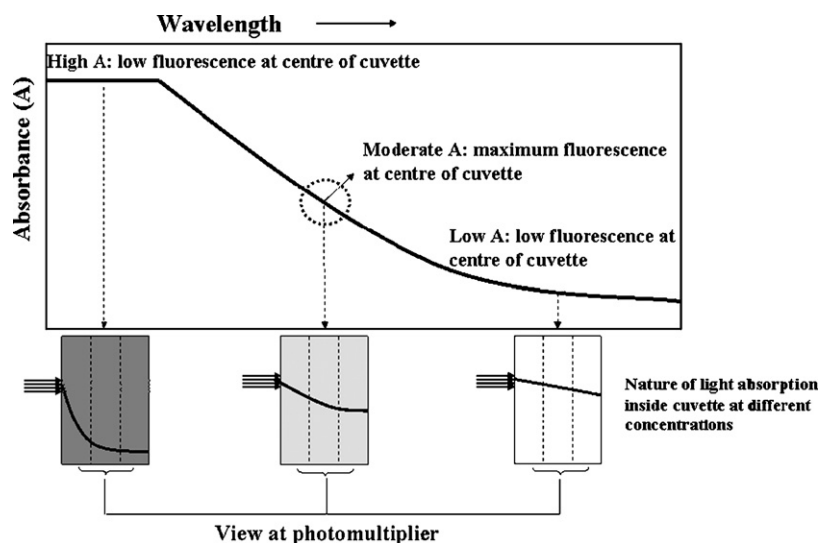
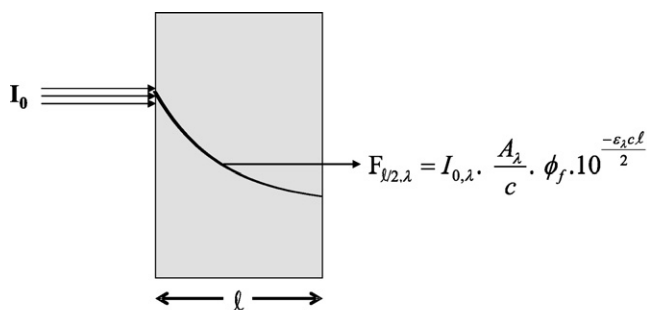


Fig. 1 – Representation of light absorption at centre of cuvette for three different conditions of absorbance of a single fluorophore.



**Fig. 2 – Illustration of light absorption in a cuvette of pathlength  $\ell$ .**

length of incident light as

$$F_{\ell, \lambda} = I_{0, \lambda} \cdot \frac{A_{\lambda}}{c} \cdot \phi_f \cdot 10^{-\epsilon_{\lambda} c \ell} \quad (5)$$

In absorption spectrometry, the variation of  $I_0$  with  $\lambda$  does not affect the absorbance measurement because a ratio of light intensities passing through the sample and the reference is measured. In fluorimetry, when an excitation or emission spectrum is scanned using spectral correction (in the corrected spectrum mode) the variation of  $I_0$  with  $\lambda$  is essentially removed. Thus, Eq. (5) can be rewritten as

$$F_{\ell, \lambda} = K \cdot A_{\lambda} \cdot 10^{-\epsilon_{\lambda} c \ell} \quad (6)$$

where  $K$  represents the constant factor ( $I_{0, \lambda} \cdot \phi_f / c$ ).

In a conventional right angle geometry, fluorescence is measured at the centre of the cuvette at  $\ell/2$  pathlength. The intensity of this fluorescence ( $F_{\ell/2}$ ), will be given by

$$F_{\ell/2, \lambda} = K \cdot A_{\lambda} \cdot 10^{-\epsilon_{\lambda} c \ell/2} \quad (7)$$

or

$$F_{\ell/2, \lambda} = K \cdot A_{\lambda} \cdot 10^{-A_{\lambda}/2} \quad (8)$$

On plotting  $A_{\lambda} \cdot 10^{-A_{\lambda}/2}$  against wavelength ( $\lambda$ ), a variation of fluorescence intensity with “ $\lambda$ ” at the centre of the cuvette (derived absorbance spectra) is obtained. For concentrated samples showing absorbance cut off as represented in Fig. 1, Eq. (8) suggests that the  $\lambda^{\max}$  of the derived absorbance spectrum ( $\lambda_{\text{der}}^{\max}$ ) is expected to give the most intense fluorescence.

In SFS, the two important parameters that characterize the spectrum are  $\Delta\lambda$  and  $\lambda_{\text{SFS}}^{\max}$ , out of which  $\Delta\lambda$  is the only independent parameter selected by the user. A particular choice of  $\Delta\lambda$ , which is often obtained by a trial method, results in a particular SFS pattern of SFS maxima. One choice of  $\Delta\lambda$  could be the difference between  $\lambda_{\text{der}}^{\max}$  (maximum of derived absorbance) and the corresponding wavelength of emission maximum ( $\lambda_{\text{der}}^{\max}$ ), which is expected to give the most intense synchronous fluorescence spectral maximum for fluorophores at higher concentrations. As concentration of the sample increases, the maximum light intensity condition at the centre of the cuvette is expected to shift to longer wavelengths. Thus, one should be able to predict the  $\lambda^{\max}$  for the SFS spectrum of concentrated

solutions using Eq. (8), by using an appropriate  $\Delta\lambda$ . The issue of the choice of  $\Delta\lambda$  in relation to Eq. (8) has been discussed later (Section 3.2.3). This expected behavior is similar to the concentration-dependent red-shift of SF spectral maximum. In this paper, the spectra generated using Eq. (8) is termed as derived absorbance plot (spectra).

### 3.2. Analysis of single fluorophores

The correspondence of Eq. (8), with the concentration-dependent shift of SFS maximum has been evaluated for some single fluorophoric samples at high concentration because the only energy degrading effect in such systems are due to inner-filter effect.

#### 3.2.1. Absorbance spectra of selected single fluorophores at high concentrations

At higher concentrations of the fluorophores, the absorbance is extremely high resulting in saturation of spectra at shorter wavelengths. The absorbance spectra at higher concentrations of the fluorophores selected for the study are given in Fig. 3. As the concentration increases the onset of the spectra get shifted to longer wavelength. Beyond an absorbance value (OD) of 2, the intensity of transmitted light is less than 1% of the incoming light and hence the data is uncertain. Therefore, absorbance values beyond 2 were given a constant value of ‘2’ and the plots were generated.

#### 3.2.2. Derived absorbance spectra of selected single fluorophores at high concentrations

At low sample concentrations, fluorescence intensity is directly proportional to absorbance. Hence, for recording a fluorescence spectra,  $\lambda_{\text{abs}}^{\max}$  ( $\lambda$  at which absorbance is maximum) of the absorbance spectrum is used, since it gives the maximum fluorescence intensity. For highly concentrated samples, selection of  $\lambda_{\text{abs}}^{\max}$  is a difficult task because of the saturation of absorption spectra (Fig. 3). With an aim to find out the excitation wavelength at which maximum fluorescence intensity can be obtained, a derived absorbance plot is generated using Eq. (8). The generated derived absorbance plots for different samples are depicted in Fig. 4.

These plots represent the variation of “ $\lambda$ ” with fluorescence intensity at the centre of the cuvette. The  $\lambda_{\text{abs}}^{\max}$  of the derived absorbance spectra can then be taken as the excitation wavelength which gives the most intense synchronous fluorescence spectra for a single fluorophoric solution at higher concentrations.

#### 3.2.3. Proposing a method for obtaining an optimal $\Delta\lambda$

For the SFS technique, the selection of wavelength interval ( $\Delta\lambda$ ) is the most important experimental parameter. However, the choice of  $\Delta\lambda$  is usually arbitrary and normally a trial method is adopted. For a typical SFS measurement, there is no general recipe for choosing  $\Delta\lambda$  that can give the best possible fluorescence intensity. The parameter  $\Delta\lambda$  is usually optimized by scanning SF spectra at various possible  $\Delta\lambda$  and selecting the one which is giving the maximum intensity (trial method). In this context, a simple method is proposed here for determining an appropriate  $\Delta\lambda$  using expression for derived absorbance maximum ( $\lambda_{\text{der}}^{\max}$ ) (Eq. (8)). Taking this  $\lambda_{\text{der}}^{\max}$  as the exciting



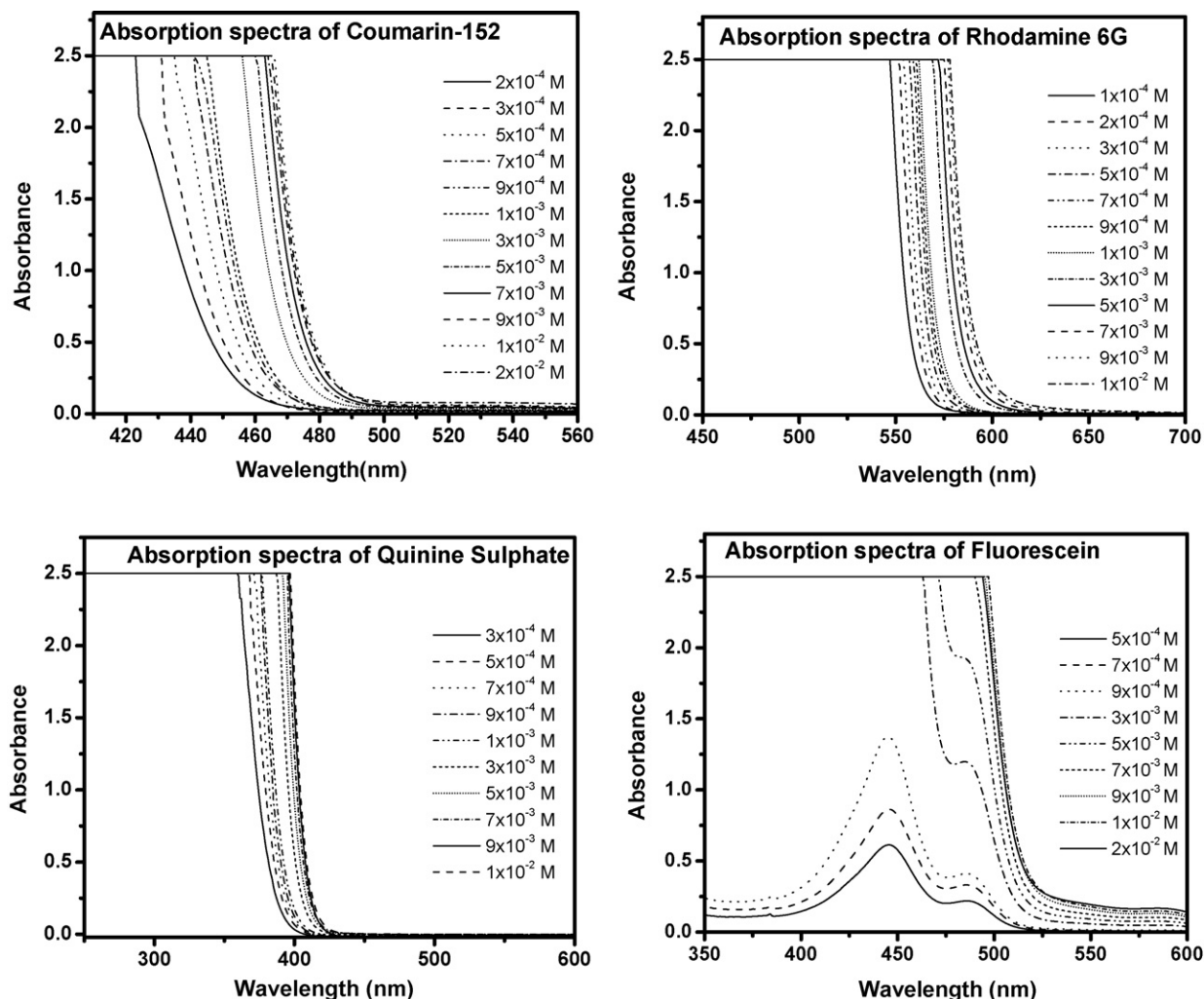


Fig. 3 – Absorption spectra of single fluorophores (coumarin 152, rhodamine 6G, quinine sulphate and fluorescein) at high concentrations.

wavelength, the emission spectrum can be recorded. The difference between the  $\lambda_{\text{em}}^{\text{max}}$  obtained from emission spectrum and  $\lambda_{\text{der}}^{\text{max}}$  of derived absorbance maximum can be considered as optimized  $\Delta\lambda$  for obtaining maximum of SFS intensity at  $\lambda_{\text{SFS}}^{\text{max}}$ . Adopting this procedure as a standardized recipe can impart a certain degree of uniqueness to the choice of  $\Delta\lambda$  for single fluorophoric solutions at high concentrations.

The SFS spectra at various  $\Delta\lambda$ s of coumarin 152, quinine sulphate, rhodamine 6G and fluorescein at high concentrations were recorded and are depicted in Fig. S2 (Supporting Information, trial method). The  $\Delta\lambda$  which gives the most intense SF spectra by trial method is found to be matching well with the  $\Delta\lambda$  by the proposed method. The  $\Delta\lambda$  values obtained by trial method and the proposed method are given in Table 1. Hence, it is evident that the  $\Delta\lambda$  obtained by Eq. (8) gives the most intense synchronous fluorescence intensity. The match of  $\Delta\lambda$  values obtained from trial method and from proposed method was not as good for rhodamine 6G as for other fluorophores. The small Stoke's shift of rhodamine 6G, and the consequent possibility of some secondary inner-filter effects being present along with the primary inner-filter effect, may explain this mismatch.

For single fluorophoric samples at high concentrations the largest value of  $\lambda_{\text{SFS}}^{\text{max}}$  is indeed obtained when a  $\Delta\lambda$  is chosen using the proposed method.

### 3.2.4. Synchronous fluorescence spectra of the selected single fluorophores at high concentrations

$\Delta\lambda$ , selected using the proposed method is used for recording the synchronous fluorescence spectra. SF spectra of the fluorophores coumarin 152, quinine sulphate, rhodamine 6G and fluorescein at high concentrations are given in Fig. S3 (Supporting Information). As the concentration increases, the SF spectral maximum gradually shifts to longer wavelengths and an explanation for this phenomenon can be given in terms of inner-filter effect.

$\lambda_{\text{der}}^{\text{max}}$  of derived absorption spectra and  $\lambda_{\text{SFS}}^{\text{max}}$  of SF spectra are plotted against the corresponding fluorophore concentration and are given in Fig. 5.  $\lambda_{\text{der}}^{\text{max}}$  of the derived absorption method and the  $\lambda_{\text{SFS}}^{\text{max}}$  of the SFS method show a very close resemblance as evident from the figures.

For single fluorophoric samples at high concentrations, the close correspondence of  $\lambda_{\text{der}}^{\text{max}}$  with  $\lambda_{\text{SFS}}^{\text{max}}$  conclusively proves

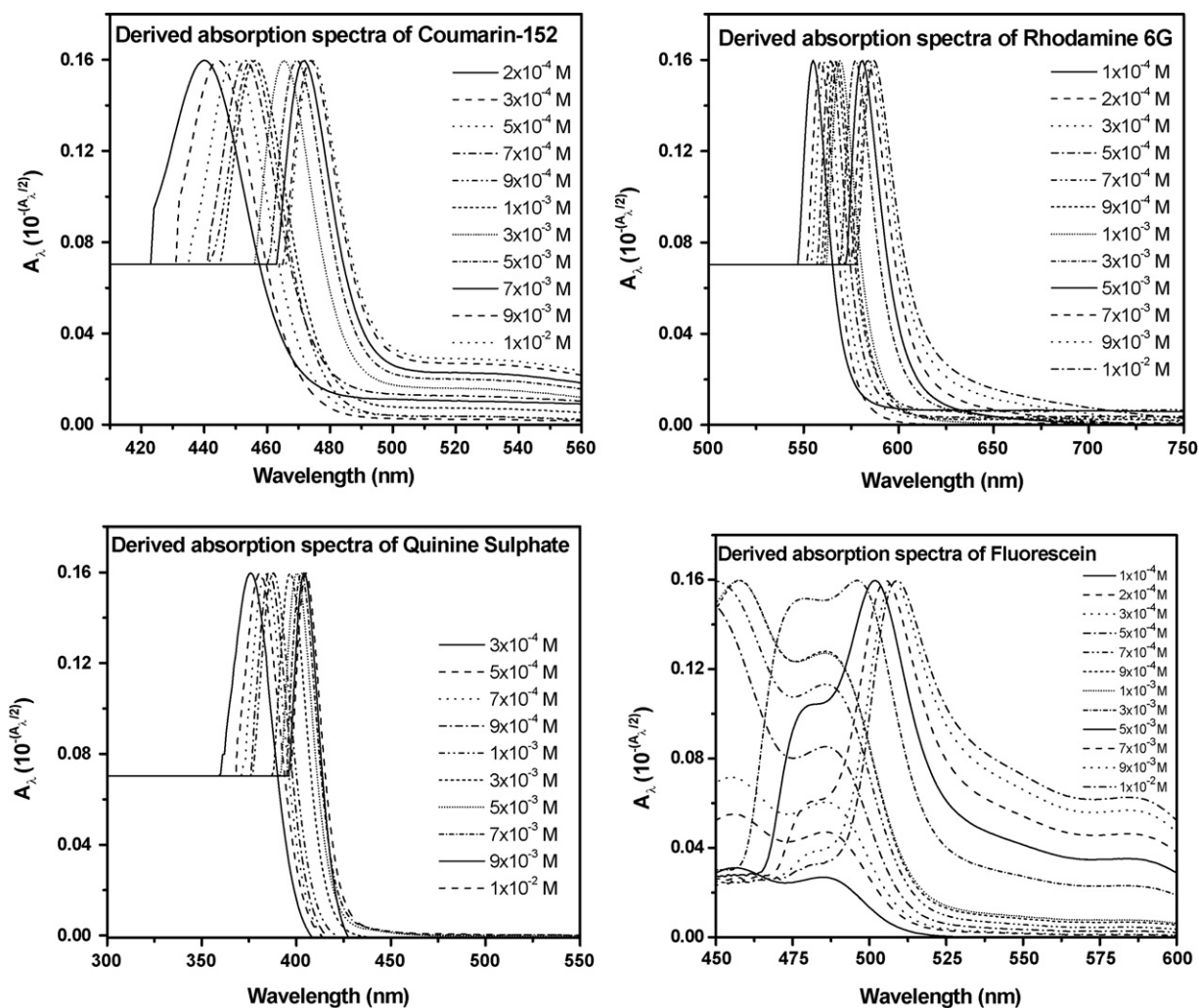


Fig. 4 – Derived absorption spectra of the selected molecules (coumarin 152, rhodamine 6G, quinine sulphate and fluorescein) at high concentrations.

Table 1 – The  $\Delta\lambda$  values obtained from proposed method (PM) and trial method (TM) of fluorophores (coumarin 152, rhodamine 6G, quinine sulphate and fluorescein) at high concentrations.

| [CONC]/M           | $(\Delta\lambda)$ |       |              |    |                  |        |             |    |
|--------------------|-------------------|-------|--------------|----|------------------|--------|-------------|----|
|                    | Coumarin 152      |       | Rhodamine 6G |    | Quinine sulphate |        | Fluorescein |    |
|                    | PM                | TM    | PM           | TM | PM               | TM     | PM          | TM |
| $1 \times 10^{-4}$ | 84                | 90    | 11           | 10 | 97               | 100    | 34          | 30 |
| $2 \times 10^{-4}$ | 75                | 70–80 | 9            | 10 | 93               | 90–100 | 34          | 30 |
| $3 \times 10^{-4}$ | 67                | 70    | 8            | 10 | 89               | 90     | 32          | 30 |
| $5 \times 10^{-4}$ | 64                | 60–70 | 6            | 10 | 84               | 80–90  | 32          | 30 |
| $7 \times 10^{-4}$ | 59                | 60    | 6            | 10 | 81               | 80     | 32          | 30 |
| $9 \times 10^{-4}$ | 58                | 60    | 6            | 10 | 79               | 80     | 31          | 30 |
| $1 \times 10^{-3}$ | 57                | 60    | 5            | 10 | 77               | 80     | 30          | 30 |
| $3 \times 10^{-3}$ | 47                | 50    | 5            | 10 | 71               | 70     | 28          | 20 |
| $5 \times 10^{-3}$ | 42                | 40    | 5            | 10 | 67               | 70     | 23          | 20 |
| $7 \times 10^{-3}$ | 41                | 40    | 5            | 10 | 63               | 60–70  | 21          | 20 |
| $9 \times 10^{-3}$ | 38                | 40    | 5            | 10 | 63               | 60     | 21          | 20 |
| $1 \times 10^{-2}$ | 38                | 40    | 5            | 10 | 61               | 60     | 21          | 20 |

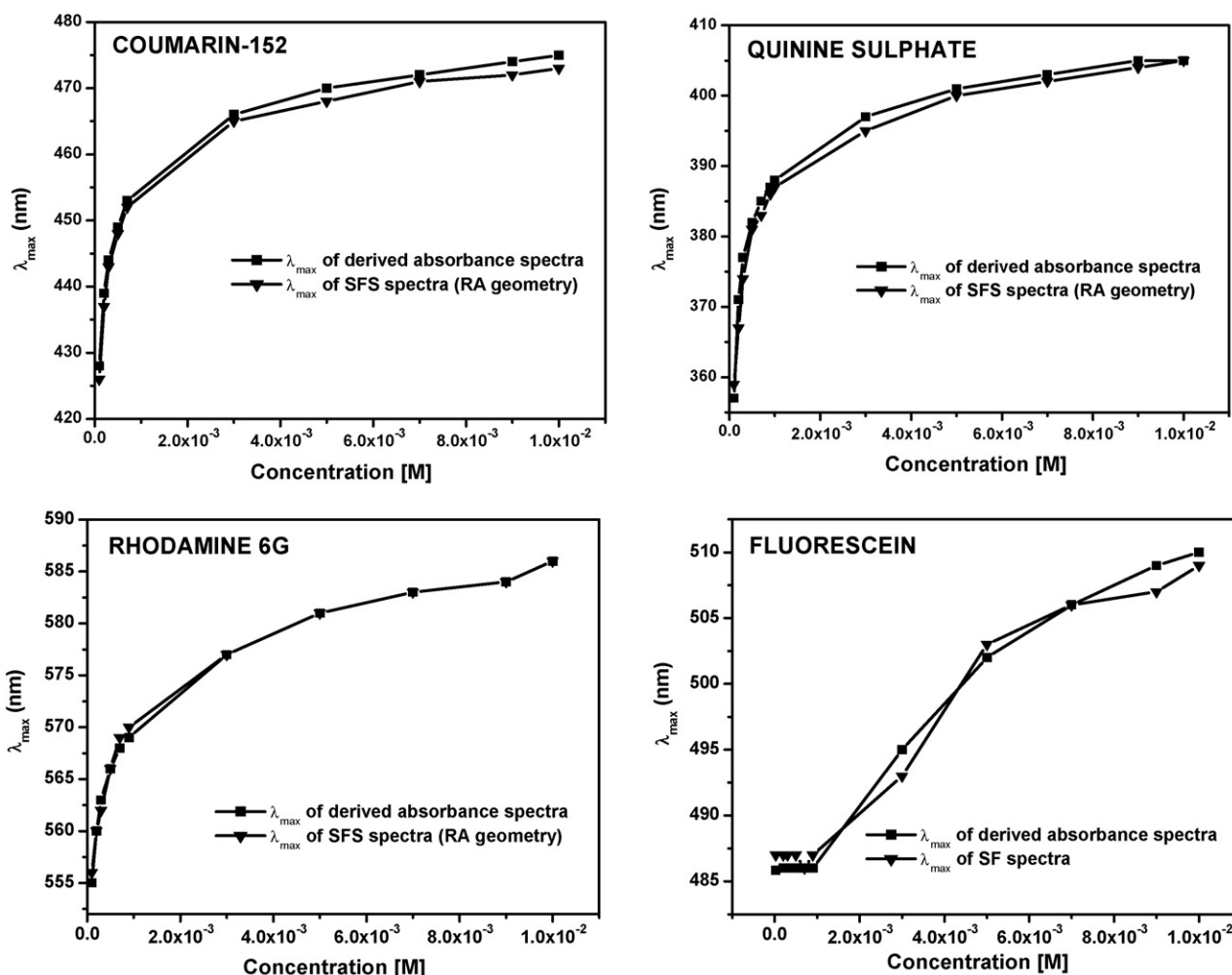


Fig. 5 – Variation of  $\lambda_{\max}^{\text{der}}$  of derived absorbance spectra and  $\lambda_{\max}^{\text{SFS}}$  of SF spectra with respect to concentration of fluorophores (coumarin 152, quinine sulphate, rhodamine 6G and fluorescein).

that the concentration-dependent red-shift exclusively originates from the inner-filter effect.

### 3.2.5. Effects of sample geometry

Generally, fluorescence is measured at right angle sample geometry. But at higher concentration of fluorophores, front surface illumination is conventionally considered preferable so as to avoid the inner-filter effect [17]. In order to understand the effect of sample geometry at high concentrations, fluorescence spectra were recorded at front face (FF) geometry as well as right angle (RA) geometry. The spectra obtained using FF and RA geometry is then compared with the derived absorbance spectra. Figs. S4 (Supporting Information) give six representative concentrations of each fluorophore.

From these figures, it is clear that the derived absorbance plot shows close correspondence with the right angle geometry spectra. It has been reported that right angle sample geometry gives a better analytical utility compared to front surface illumination and  $45^\circ$  sample geometry for the analysis of petroleum fuels and their mixtures at higher concentration [7]. Kao et al. also observed that, right angle geometry

exhibits the widest linear dynamic range [14]. Hence, it is obvious that synchronous fluorescence spectroscopic analysis of single fluorophoric samples at high concentrations is more advantageous when a right angle sample geometry is adopted.

In short, for single fluorophoric systems at high concentrations when there is no other energy degrading interactions among the fluorophores and the quantum efficiency is independent of the excitation wavelength, inner-filter effect is the only operating mechanism causing the concentration-dependent red-shift and the proposed method is well applicable.

### 3.3. Applying the proposed method for multifluorophoric samples

The absorption spectra of various dilutions of diesel, transformer oil and humic acid are depicted in Fig. S5A, Fig. S6A and Fig. S7A, respectively (Supporting Information). It is seen that the saturation behavior of the longer wavelength edge of the absorption spectra of these multifluorophoric systems at high concentrations is same as

that of the single fluorophores at high concentrations. Thus, inner-filter effect is expected to play a significant role in determining the extent of concentration-dependent red-shift in synchronous fluorescence spectra of multifluorophoric samples too. Hence, the applicability of the derived Eq. (8) and the proposed method can also be evaluated for multifluorophoric systems.

It is to be noted that the photo-physical properties of multifluorophoric samples at high concentrations are different from those of single fluorophoric samples at high concentrations. The crucial assumption for deriving Eq. (8) was that quantum yield is independent of the excitation wavelength. In most of the multifluorophoric systems at higher concentrations, the quantum yield is excitation wavelength dependent. This is in contrast to the case of single fluorophoric samples at high concentrations where the quantum yield is independent of the excitation wavelength. In addition, energy degrading interactions present in multifluorophoric systems at high concentrations results in the modifications of quantum yield (either enhancement in quantum yield due to resonance energy transfer or reduction in quantum yield due to flu-

orescence quenching) and due to excimer and/or exciplex formation, new emissions may appear at the expense of emission at other wavelengths (monomer emission). Hence, the one-to-one correspondence of the derived absorbance maxima and the synchronous fluorescence maxima, as observed for single fluorophores at high concentrations, is not expected to be observed for multifluorophoric samples at high concentrations.

However, if the relative contributions of the above energy degrading and intensity modifying effects are less important compared to the inner-filter effect, the proposed method can still be an useful technique in understanding the concentration-dependent red-shift of multifluorophoric samples and it could be applied for uniquely selecting a  $\Delta\lambda$  that can result in maximum fluorescence at  $\lambda_{\text{SFS}}^{\text{max}}$ . As observed earlier, although not carried out in this work, fluorescence lifetime measurements would be of great help in this regard.

Two different groups of multifluorophoric samples were selected for this study: (i) A system wherein generally all the absorbing molecules are fluorescent (e.g. polycyclic aromatic hydrocarbons (PAHs) in diesel and transformer oil).

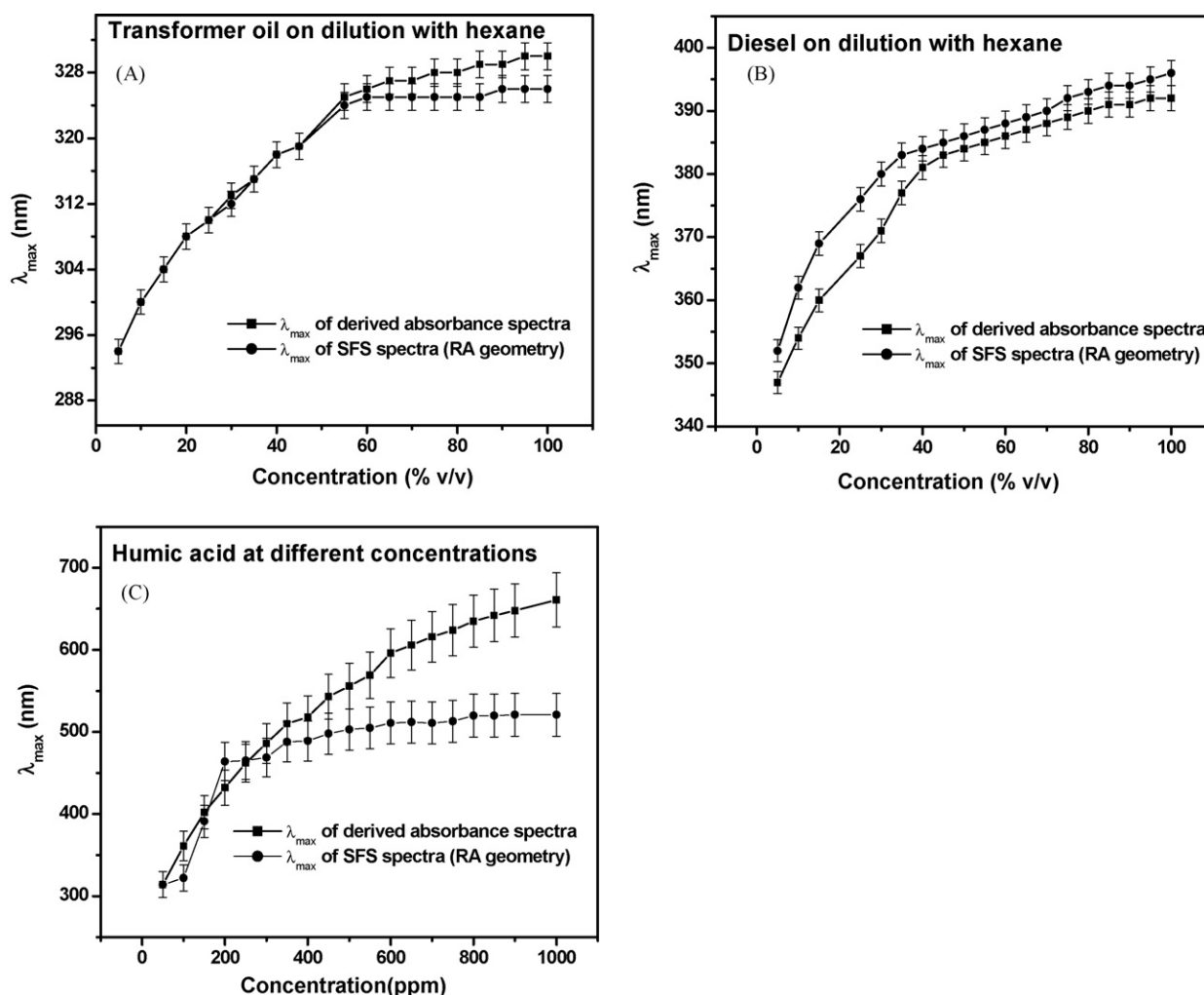


Fig. 6 – Correspondence of  $\lambda_{\text{max}}^{\text{der}}$  of derived absorbance spectra with  $\lambda_{\text{SFS}}^{\text{max}}$  of SF spectra (RA geometry) of (A) diesel samples on dilution with hexane, (B) transformer oil samples on dilution with hexane and (C) humic acid samples on dilution with water.



(ii) A system wherein some of the absorbing molecules are fluorescent (e.g. humic acid). The proposed method for finding optimal  $\lambda_{\text{SFS}}^{\text{max}}$  and  $\Delta\lambda$  were then applied for these samples.

For diesel samples diluted by hexane, using Eq. (8), the derived absorption spectra were generated and are given in Fig. S5B (Supporting Information). By choosing  $\lambda_{\text{der}}^{\text{max}}$  of the derived absorbance plot as  $\lambda_{\text{ex}}$ , an appropriate  $\Delta\lambda$  is selected. Using this  $\Delta\lambda$ , synchronous fluorescence spectra (right angle geometry) were recorded and are shown in Fig. S5C (Supporting Information). The  $\lambda_{\text{SFS}}^{\text{max}}$  of SF spectra show a gradual red-shift as the concentration increases. The correspondence of the derived absorbance ( $\lambda_{\text{der}}^{\text{max}}$ ) and synchronous fluorescence ( $\lambda_{\text{SFS}}^{\text{max}}$ ) can be easily observed from Fig. 6A. The close correspondence of the values suggests that the proposed method is well applicable for diesel samples.

Different concentration of transformer oil samples were prepared by diluting with hexane. For transformer oil samples, the derived absorbance spectra obtained using Eq. (8) are given in Fig. S6B (Supporting Information). Using the derived absorbance maxima ( $\lambda_{\text{der}}^{\text{max}}$ ),  $\Delta\lambda$  is selected and the corresponding SF spectra were generated (Fig. S6C, Supporting Information). The derived absorbance maxima ( $\lambda_{\text{der}}^{\text{max}}$ ) and SF spectral maxima ( $\lambda_{\text{SFS}}^{\text{max}}$ ) shows good correspondence for transformer oil samples as evident from Fig. 6B.

For humic acid samples of various dilutions, the derived absorption spectra and the synchronous fluorescence spectra are shown in Fig. S7B and C, respectively (Supporting Information). The maximum of the derived absorbance ( $\lambda_{\text{der}}^{\text{max}}$ ) spectra and synchronous fluorescence ( $\lambda_{\text{SFS}}^{\text{max}}$ ) spectra are plotted against concentration and are depicted in Fig. 6C.

At high concentrations the close correspondence between the  $\lambda_{\text{der}}^{\text{max}}$  and  $\lambda_{\text{SFS}}^{\text{max}}$  is lacking which implies that Eq. (8) is not valid for the humic acid system.

The correspondence between  $\lambda_{\text{der}}^{\text{max}}$  and  $\lambda_{\text{SFS}}^{\text{max}}$  essentially signifies that inner-filter effect is the predominant cause for the concentration-dependent red-shift, which is true for diesel and transformer oil, where most of the chromophores absorbing in the spectral range of interest are fluorophores too. The mismatch of  $\lambda_{\text{der}}^{\text{max}}$  and  $\lambda_{\text{SFS}}^{\text{max}}$  in the case humic acid sample probably originates from the possibility that all the chromophores absorbing light are not fluorophores and in such a case, self-quenching at higher concentrations can be very significant. Immediate saturation of  $\lambda_{\text{SFS}}^{\text{max}}$  in humic acid samples essentially indicates the very high level of self-quenching at higher concentrations.

Following conventional wisdom, front face (FF) geometry has been the preferred mode for fluorescence measurements on samples at high concentrations [10,11]. However, in a study involving nitrofluorene and anthracene, Kao et al. showed that right angle geometry gives a good linear dynamic range and analytical utility compared to other sample geometries [14]. In a detailed investigation on the significance of sample geometry in the analytical fluorimetry of multifluorophoric samples at high concentrations, Patra and Mishra have shown that the right angle geometry shows greater sensitivity to concentration-dependent red-shift of the SFS of petroleum products [7,8].

Hence, we have adopted front face as well as right angle geometry for the synchronous fluorescence analysis of the above mentioned multifluorophoric systems at high concentrations. The  $\lambda_{\text{der}}^{\text{max}}$  of derived absorption spectra,  $\lambda_{\text{SFS}}^{\text{max}}$  of SF spectra at front face geometry are plotted against concentration for diesel and transformer oil samples.

It has already been shown in Fig. 6A and B that the SF spectra at right angle geometry show a close correspondence with the derived absorbance maxima. From Fig. S8 (supporting Information) it is evident that there is no correspondence between the derived absorbance maxima ( $\lambda_{\text{der}}^{\text{max}}$ ) and synchronous fluorescence maxima (FF geometry) which essentially suggests that when inner-filter effect is the major reason for concentration-dependent red-shift, right angle geometry is a preferred choice over front face geometry.

Results of all the investigation using transformer oil, diesel and humic acid are summarized in Tables S1, S2 and S3, respectively (Supplementary information).

The  $\Delta\lambda$  values for diesel samples (neat diesel to 5% diesel in hexane) varies from 37 nm to 54 nm. Patra et al. have used a value of  $\Delta\lambda$ , 40 nm for analytical applications involving diesel-kerosene mixtures by a trial method [6]. The range of  $\Delta\lambda$  (37–54 nm for diesel samples) variation that has been obtained through this analysis provides a rationale for the choice of  $\Delta\lambda$  40 nm.

Hence, the proposed method can be well applied for multifluorophoric systems where almost all the chromophores are fluorescent. A close correspondence of  $\lambda_{\text{SFS}}^{\text{max}}$  and  $\lambda_{\text{der}}^{\text{max}}$  values provide evidence that the major cause of concentration-dependent red-shift is inner-filter effect. The deviation of  $\lambda_{\text{SFS}}^{\text{max}}$  from  $\lambda_{\text{der}}^{\text{max}}$  clearly show that the proposed method is not applicable for systems where not all the chromophores are fluorescent. In short, mismatch of the  $\lambda_{\text{der}}^{\text{max}}$  of the derived absorbance method (predicted red-shift) and  $\lambda_{\text{SFS}}^{\text{max}}$  of the synchronous fluorescence method (observed red-shift) can give vital clues with regard to the nature of the multifluorophoric systems.

### 3.4. Conclusions

Conventionally, the concentration-dependent red-shift of fluorescence in multifluorophoric solutions at high concentrations has been explained in terms of energy degrading mechanisms like energy transfer, excited state bimolecular interactions and quenching. However, the present work shows that the major contributing cause for this effect is the inner-filter effect, especially under right angle sample geometry conditions. For concentrated samples with saturating absorption, a derived absorbance plot seems to correlate well with the observed synchronous fluorescence spectra. Using this derived plot, a method has been proposed which enables obtaining a  $\Delta\lambda$  that can give maximum fluorescence at  $\lambda_{\text{SFS}}^{\text{max}}$ . Currently, the synchronous spectral conditions of a multifluorophoric system are optimized using a trial method. This work suggests that the proposed method can be a standardized recipe for obtaining synchronous fluorescence spectra of concentrated multifluorophoric samples.

---

## Acknowledgements

The authors thank the Council of Scientific and Industrial Research (CSIR) New Delhi for financial assistance. Divya thanks CSIR New Delhi for a fellowship.

---

## Appendix A. Supplementary data

Supplementary data associated with this article can be found, in the online version, at [doi:10.1016/j.aca.2008.09.056](https://doi.org/10.1016/j.aca.2008.09.056).

---

## REFERENCES

- [1] C.A. Parker, W.T. Rees, *Analyst* 87 (1962) 83.
- [2] C.A. Parker, *Photoluminescence of Solutions*, Elsevier Publishing Company, Amsterdam, 1968.
- [3] M.C. Yappert Jr., J.D. Ingle, *Appl. Spectrosc.* 43 (1989) 759.
- [4] R.A. Leese, E.L. Wehry, *Anal. Chem.* 50 (1978) 1193.
- [5] P. John, I. Soutar, *Anal. Chem.* 48 (1976) 520.
- [6] D. Patra, K.L. Sireesha, A.K. Mishra, *J. Sci. Ind. Res.* 59 (2000) 300.
- [7] D. Patra, A.K. Mishra, *Analyst* 125 (2000) 1383.
- [8] D. Patra, A.K. Mishra, *Talanta* 53 (2001) 783.
- [9] X. Wang, O.C. Mullins, *Appl. Spectrosc.* 48 (1994) 977.
- [10] T.D. Downare, O.C. Mullins, *Appl. Spectrosc.* 49 (1995) 754.
- [11] C.Y. Ralston, X. Wu, O.C. Mullins, *Appl. Spectrosc.* 50 (1996) 1563.
- [12] G.C. Smith, J.F. Sinski, *Appl. Spectrosc.* 53 (1999) 1459.
- [13] J.F. Sinski, B.S. Compton, B.S. Perkins, M.C. Nicoson, *Appl. Spectrosc.* 58 (2004) 91.
- [14] S. Kao, A.N. Asanov, P.B. Oldham, *Instrum. Sci. Technol.* 26 (1998) 375.
- [15] D. Patra, K.L. Sireesha, A.K. Mishra, *Indian J. Chem. A.* 40A (2001) 374.
- [16] D. Patra, A.K. Mishra, *Anal. Bioanal. Chem.* 373 (2002) 304.
- [17] D. Patra, A.K. Mishra, *Spectrosc. Lett.* 35 (2002) 125.
- [18] D. Patra, A.K. Mishra, *Anal. Chim. Acta* 454 (2002) 209.
- [19] D. Patra, A.K. Mishra, *Appl. Spectrosc.* 55 (2001) 338.